A comparative Analysis of Grain Size distributions and Cross Sections using an Oblique Photoset on the Nisqually Riverbed Adjacent to Longmire In Mount Rainier National Park

Austin Rains

A report prepared in partial fulfillment of
the requirements for the degree of

Master of Science
Earth and Space Sciences: Applied Geosciences

University of Washington

March 2019

Project mentor:
Taylor Kenyon, Mount Rainier National Park

Internship coordinator:
Kathy Troost

Reading Committee:
Juliet Crider
Steven Walters

MESSAGe Technical Report Number: [072]

Abstract

Collecting cobble counts and gathering cross sections out in the field can be a tedious and time consuming process. An attempt was made at expediting this process using structure from motion technology to create an orthophoto and a digital surface model of the Nisqually riverbed adjacent to Longmire in Mount Rainier National Park. An oblique photoset was gathered of the Nisqually riverbed using a telescoping pole with a digital camera and high-precision GPS mounted at the end of it. This photoset was then used to create a point cloud, an orthophoto, and a digital surface model using Pix4D. Automated cobble counts were gathered using two different Matlab scripts; DigitalGrainSize, and BASEGRAIN. DigitalGrainSize proved to be fairly accurate and may act as a replacement if grain sizes 11 mm and below are not relevant to a study. An automated grain size distribution may be even more accurate if a higher resolution digital surface model is produced or if a single photo is used instead of an orthophoto. BASEGRAIN did not perform as well and did not detect both smaller and larger grain sizes. Cross sections were derived from the digital surface model and have a high resolution when compared to 1 m resolution lidar in the same area. Channels that are only active at higher flows can be seen clearly in the digital surface model cross sections as well. The only drawbacks are that vegetation, and water are included in the digital surface model, so it cannot measure beneath the water's surface as opposed to a total station, and the elevation was approximately 60 feet lower than actual elevation. This was likely due to a GPS error. I believe that these two applications show promise, especially if these techniques are refined.

Acknowledgments

There is a long list of people that have made it possible for me to complete this project. Thanks to Taylor Kenyon and Robbie Jost, Mount Rainer National Park, for getting me started on this work and giving me the idea for the project. I would like to thank Professor Juliet Crider for her insight and guidance from the start, as well as her exceptional editing and proofreading. I would also like to thank Professor Steven Walters for his proofreading and support on the technical side of things. Mary Alice Benson is responsible for helping collect field data and data collection would not have been possible without her. The equipment used for data collection was lent to me by Professor David Shean, UW Civil & Environmental Engineering, and improved the quality of my dataset. Lastly, I would like to thank my professors and peers in MESSAGe. Without their support and guidance, this path would have been much more difficult.

Table of Contents

1.0 Introduction

1.1 Purpose and Scope

The purpose of this investigation is to compare grain size distributions and cross sections created using photogrammetry with grain size distributions produced with manual cobble counts and cross-sections taken from a ten-year-old lidar dataset. The study site is a reach of the Nisqually River at Longmire, in the southwest corner of Mount Rainier National Park, Washington. This project was suggested by the Park's "Imminent Threats" technicians, Taylor Keyon and Robert Jost. Deglaciation of the headwaters of rivers sourced at Mount Rainier has released significant volumes of sediment that migrate downstream and pose a hazard to Park infrastructure. The Imminent Threats Team is charged with identifying and monitoring such hazards. Channel cross sections and grain size distributions in the active channel provide data to document sediment aggradation and the migration of sediment bulges. This project is motivated by the observation that photogrammetry is less expensive to collect than lidar and may be less time consuming than conducting cobble counts across an entire reach of the river. If the photogrammetric methods can produce grain size distributions and cross sections that are comparable to the other methods, Park technicians can then use photogrammetry throughout the Park to replace the more time consuming parts of field work, and perhaps also increase the frequency of surveys, to monitor aggradation and anticipate flooding of the rivers. Photogrammetric surveys have the potential to sample a broader area of a reach than the small sections or transects typically sampled by cobble counts. Even if the data aren't as accurate as manual cobble counts or lidar, the orthophotographs and digital surface models that are generated may help Park technicians examine broader features, such as sediment bulges, and the rapidly changing morphology of the Nisqually River.

1.2 Site Location

The field site chosen for this investigation is a reach of the Nisqually River adjacent to Longmire, located in the southwest quadrant of Mount Rainier National Park (Fig. 1). This site is approximately five miles downstream of the Nisqually Glacier and 20 miles upstream from Alder Lake Reservoir. The site also located right next to the building that houses the imminent threats team. This location gives easy access to both banks of the Nisqually because of a bridge at the site. The site from the south bank can be seen in figure 2.

This site works well for this investigation for a few reasons. There are annual cobble count data available from consecutive UW field courses in September 2012-2018. Although slightly inconsistent in methods each year, these data are used as the reference to compare against grain size distributions determined with photogrammetry. There is also 1m lidar coverage at this site from October 2007 that can be used to compare with cross sections from the DSM. It is also a site of regular channel cross-section surveys by the Park.

1.3 Background

1.3.1 Local Geology

The upper reaches of the Nisqually River is within Mount Rainier National Park. Mount Rainier is a ~500ky, dominantly andesitic stratovolcano (Sisson and Valance, 2001). The mountain range on the south side of the park is the Tatoosh Range composed of 26-12 Ma granodiorite

(Mattinson, 1977). The Tatoosh Pluton is the remnant of a volcanic system that penetrated the Ohanapecosh Formation and supplied volcanoes that came before Mount Rainier (Fiske, et al., 1963). Some other units found in the Park are older volcanic arc rocks such as the Ohanapecosh Formation that were formed during subaqueous eruptions (Fiske, et al., 1963).The youngest units are mudflows, pyroclastic flows, and tephra deposits (Fiske, et al., 1963). The rock types most commonly found in the Nisqually River channel are granodiorite from the Tatoosh Range and andesite supplied from Mount Rainier.

1.3.2 Geomorphology

There is a combined total of 29 named glaciers on Mount Rainier and in total, cover 30.41 mi^2, or 31.21 mi^2 if perennial snow fields are included. In terms of volume, Mount Rainier has 1.06 cubic miles of ice. Rainier has more ice on it than on all of the other Cascade volcanoes combined (Driedger and Kennard, 1986). Overall, the glaciers on Mount Rainier are currently in a state of retreat (Beason, 2017). From 1896 to 2015, Mount Rainier has lost 20.11 mi^2 of ice coverage (Beason, 2017). These glaciers supply water and sediment to several major rivers around the volcano.

The Upper Nisqually River is fed by the Nisqually Glacier, one of the largest glaciers on Mount Rainier's south face. The Nisqually Glacier, as with the other glaciers in the Park, is currently in a state of retreat (Beason, 2017), releasing sediment that has been trapped in the ice. This sediment is being transported and deposited by the Nisqually River, causing aggradation in the channel. As the Nisqually Glacier retreats, steeper terrain is exposed. These steep angles are above the debris flow initiation threshold, which would increase debris flow activity (Legg, et al., 2014). As long as the climate continues to warm and the glaciers retreat, more sediment will be introduced to channels, causing aggradation and disequilibrium in rivers around the Park (Legg, et al., 2014).

The Nisqually River watershed at Longmire is fed by the Nisqually Glacier, Van Trump Creek, and Paradise River. The total area of the watershed is 18.79 $miles^2$ (Beason, et al., 2015) This watershed includes the summit of Mount Rainier at 4,392 m above sea level (a.s.l.), to Longmire at 831 m a.s.l. This makes the average gradient of the Nisqually between these points 3.36% (Beason, et al., 2015).

The channel of the Nisqually near Longmire is relatively narrow as it is confined by intrusive rocks on each bank. Just after the Longmire Bridge, the river begins to widen from 40 meters to 100 meters, just 200 meters downstream of the bridge (Figure 1).

1.3.3 Imminent Threats

Mount Rainier National Park is replete with geological threats to the Park infrastructure, including short term rock fall, debris flows, flooding, glacial outburst floods, and landslides (Beason et al., 2015). This list does not include catastrophic events such as volcanic eruptions or collapse, due to their long recurrence intervals (Beason et al., 2015). Debris flows are particularly common. They are created from subglacial outburst floods, otherwise known as jökulhlaups. Jökulhlaups are created during periods of high temperatures as meltwater becomes trapped beneath a glacier and is then released abruptly. Most commonly though, debris flows in Mount Rainier National Park are caused by heavy rains from winter storms or warming

temperatures in the spring or summer (Beason et al., 2015). One way of monitoring the amount of aggradation or incision caused by these debris flows is by doing yearly cross sections in the river channels. These cross sections can gauge whether a river is being aggraded, incised, or is at equilibrium. Surveys done over the years in the Park have determined that all rivers are aggrading despite heavy floods in the last few decades (Beason, et al., 2015). Understanding these rates of aggradation is integral to predicting the future of the Park's rivers (Beason, et al., 2015).

The Nisqually River is one of the rivers in the Park that has been affected by receding glaciers and heavy debris flows. It also borders one of the most important roads in the Park and passes adjacent to Longmire, a small village that houses Park staff, Park maintenance, and tourist facilities. In recent decades several debris-flow events have damaged roads, bridges and facilities in the southwest corner of the park. The most damaging events happened during the Nov. 2006 storm. During the 2006 flood event, there was an avulsion along the Kautz River, a mile upstream from the Nisqually – Paradise Road (Bullock, et al., 2007). When the Kautz River avulsed, it flowed over the Nisqually – Paradise road, 200 yards east of the Kautz Creek Bridge (Bullock, et al., 2007). Slightly to the west, the Tahoma Creek Bridge is in danger of being destroyed. The aggradation of Tahoma Creek is so rapid, that the channel must be dredged every second year, which is costly for the Park. There is concern that a debris flow flood can wash out the Tahoma Bridge because there is little clearance between the river and the base of the bridge. According to Anderson, et al. (2013), even moderate aggradation could wash out the bridge. In 2006, the same flood destroyed Sunshine Point, a campground near the west entrance of the park. It also nearly took out the emergency operations center in Longmire (Figure 3).

The reach of the Nisqually examined in this study is adjacent to Longmire where sediment aggradation has been observed as well as incision and remains in slight equilibrium (Beason, et al., 2015). The elevation of the Nisqually River channel adjacent to Longmire is actually higher than most of Longmire (Beason, et al., 2015). To prevent flooding, the Park constructed a levee on the right bank of the river (Beason, et al., 2015). It would require a large flood to overtop this levee (Beason, et al., 2015). Longmire, along with the Nisqually River and levee dividing them can be seen with Longmire being at a lower elevation than the river in Figure 4.

The goal of my analysis is to evaluate methods intended to streamline efforts to monitor grain size distribution, channel profiles and channel indicate changes in the Nisqually River channel and other channels in the Park. It is important to monitor these rivers as they try to find equilibrium between aggradation and incision. In this report I consider whether and how ground-based digital photos can provide quantitative information on these attributes.

2.0 Methods and Materials

New tools in digital photogrammetry allow generation of orthorectified photographs (orthophoto) and high-resolution digital surface model (DSM) of the channel reach. An overview of the whole process includes gathering a photoset with a camera attached to a high precision GPS, creating a point cloud with that photoset, creating an orthophoto and DSM with that point cloud, and then using GIS and Matlab to get cross sections and automated grain size distributions. There are a few intermediate steps that are needed to convert files and such. The

derived cross sections and grain size distributions are then compared with cross sections gathered from lidar and grain size distributions from manual cobble counts.

2.1 Data Collection

2.1.1 Ground-based photography for photogrammetry

The first step is to gather a photoset for analysis in structure-from-motion photogrammetry. Cloudy days provide the best conditions under which to gather a photoset being used to create an orthophoto and DEM, minimizing the effects of shadows in the photos. When gathering the photoset, it is also important to use a telescoping pole to give the photos less "obliqueness" and more of a view of what is behind objects in the field of view. In an ideal situation, an unmanned aerial vehicle (UAV) would be used to gather a photoset because that would eliminate any obliqueness, but since UAVs are not allowed in national parks, a telescoping pole is the next best thing. If the photos are too oblique, there is a "ray" effect and objects are stretched and distorted, which can affect final results. The camera used for this project is a remotely triggered Sony NEX-5 camera. The remotely triggered aspect requires two people but allows one user to hold the telescoping pole while the other uses the remote. Another piece of equipment that is very helpful is a high-precision GPS mounted on the camera. This step geolocates each photo, making it easier for the structure-from-motion software to align the photos. Though not completely necessary, the combination aligns more photos and acts as a ground control for the DEM and orthophoto. The specific GPS used for this project is am Emlid Reach GNSS receiver that was jerry-rigged on top of the camera. This GPS unit has centimeter grade accuracy. An important aspect to consider when gathering the photoset is that the photos need to have around 70% overlap so that the structure-from-motion software is able to align them properly. The best way to do this is to have an organized approach to shooting the photos. For this project, most photos were taken facing upstream. The camera faced the same direction every photo, with every photo taken a few meters to either side of the preceding photo. This creates a zig-zag pattern that can be seen in Figure 5. The total time spent setting up equipment and collecting photos is about 5 hours, but this also depends on the scale of the project. Originally I had included coded targets provided by Agisoft, but I did not end up using Agisoft so that step can be skipped. As far as I know, the coded targets had little effect on aligning photos in Pix4D.

2.1.2: Digital photogrammetry with commercial software

The next step after the photoset is collected is to run the photos through a structure-from-motion (SfM) program. This software is used to produce a point cloud comparable to lidar (Figure 6); an orthorectified photograph (orthophoto), which is an un-distorted photomosaic; and a digital surface model (DSM) to model the terrain. Structure-from-motion uses a series of overlapping images to create a database full of unique features found in the photos and then it estimates the geometry of whatever object is in the photos along with trying to estimate camera positioning (Snavely, 2008). To help align the photos, GPS coordinates can be inputted for each photo, helping the program estimate camera positioning. In the Department of Earth and Space Sciences (ESS), we currently have access to two SfM software packages: Pix4D (Pix4D, version 4.4.4) and Agisoft Photoscan (Agisoft, Version 1.4.4). Both of these programs work well and can produce what is needed for the project, but I decided to use Pix4D. First, Pix4D is much more user friendly than Agisoft. All that is needed to create the models is to plug in the photos, the GPS coordinates, and then select the parameters that are desired, and then the program will

create them all in one step. Agisoft has more of a learning curve and can be confusing. It also does not allow you to create the models in one step, and an individual must be available to do some clicking to start the separate steps. Second, Pix4D also consistently produced better results for the type of terrain I am modeling. When using Agisoft, the channel was distorted and several different channels on different planes were created, and I did not have this problem using Pix4D. Running the photogrammetry software is probably the most time-intensive step, depending on the required resolution of the dense cloud, DSM, and orthophoto. To produce the point cloud, I did not need to do any editing of the raw photos. I could have masked out the water, but this would have been a time-intensive step and I would not have captured the elevation of the water's surface if I had masked it out.

2.1.3 Digitally-Derived Grain Size Distributions

Scientists have been trying to estimate grain size distributions with automated techniques since the early 2000's using a number of different methods. One of the first methods used a texture analysis of airborne photographs (Carbonneau, et al., 2004), or doing a texture analysis of terrestrial laser scans (Heritage and Milan, 2009). The two programs used in this study are DigitalGrainSize (DGS) (Buscombe, 2013) and BASEGRAIN (Detert and Weitbrecht, 2012). Each program uses MATLAB as the interface and processing engine, but they use different methods of detecting grains as explained above. BASEGRAIN uses a grayscale threshold approach and binary images where single grain elements are separated by interstices (Weichert et al., 2004). DGS does a frequency analysis of 8-bit grayscale images (Buscombe et al., 2010). DGS uses wavelets while BASEGRAIN uses a five-step object detection algorithm that separate interstices from grain areas.

To get a grain size distribution and cross section using photogrammetry requires several steps.

1. Gather a photoset with a digital camera and high-precision GPS (above)
2. Extract GPS data, run photoset though a structure-from-motion program. (Pix4D, Agisoft Photoscan) and create both an orthophoto and DSM (digital surface model)
3. Extract sample areas from the orthophoto and extract cross-sections from the DSM using ArcMap
4. Use Adobe Photoshop to convert image files into the correct format
5. Run the images though both DGS and BASEGRAIN
6. Plot data in Microsoft Excel

Once an orthophoto and DSM were produced, I used Esri ArcMap to mask out the specific areas from which to extract the grain size distribution, for direct comparison with field-based cobble counts. From the orthophoto, I selected six sample areas (Figure 7) on which to conduct automated cobble counts. The idea is that if I used six sample areas, I could average the results in case there were some outliers. I had to make sure that I masked out areas large enough to get a big enough sample size for DGS and BASEGRAIN. For the DGS method, a minimum sample size is approximately 100 grains (Buscombe, 2010), and for BASEGRAIN, the minimum sample size is approximately 150 grains with at least 30 of those grains being medium grain size fractions (Detert and Weitbrecht, 2012).

After the areas were masked, the photos were refined in Adobe Photoshop. DGS requires the photos to be in a specific format: is 8-bit, grayscale, JPEGs. For BASEGRAIN, there is no

required format, so I used the same format that was used for DGS. I used Photoshop to convert the TIFFs derived from ArcMap to the specific format. Photoshop also allowed me to crop the photos into perfect squares, which are required for accuracy.

After the photos are prepared, they were then run through DGS or BASEGRAIN scripts in MatLab. The scripts each created a graphic user interface that allows the user to load, filter, and flatten images. It also allows the user to set a "millimeters per pixel" scale so that the size of grains can be determined. After the parameters are set, a grain size distribution is gathered automatically. DGS output includes grain size bins, the percent of grains in that bin, and the grain size at certain percentiles (D50, D84). BASEGRAIN output includes much of the same but also includes extra information that was not used for this project. Key differences between the scripts are that DGS uses a frequency analysis algorithm to detect grains (Buscombe, 2010) while BASEGRAIN does a five-step analysis on single-grain elements separated by interstices (Detert and Weitbrecht, 2012).

To plot the data for comparison with field-based cobble counts, I took the raw data from both DGS and BASEGRAIN and plotted it in Excel. I first made two graphs displaying each the DGS results, with a composite graphed, and did the same with BASEGRAIN. I then plotted the D50 and D84 resulting from both programs onto a graph to compare them to each other. Lastly, I plotted the composite grain size distributions from both programs alongside the manual cobble counts and did the same with the D50 and D84. To make an accurate comparison between the automated and manual counts, I truncated the data of the automated counts. This meant only using grain sizes of 9 mm to 320 mm since that is the range of manual cobble counts.

2.1.4 Manual Cobble Counts

To compare with the digital grain size data, I used field data collected in an annual class projects by students in the MESSAGe September field course. Each MESSAGe cohort used the Wolman pebble count method (Wolman, 1954). To perform the Wolman Method, one needs a measuring tape and a gravelometer, an aluminum grid with a range of square openings. A transect is made with the measuring tape, and every half meter, an individual reaches down, without looking, and picks up whatever grain their finger touches. The intermediate axis is then measured with a gravelometer. The smallest hole that a grain could fit through is considered its grain size. This is done to at least 100 different grains. The limitation with the Wolman Method is that grain less than 2 mm cannot be measured; however, this is not problematic because fines are discounted for automated grain size distributions.

I collected cobble counts in September 2018 with cohort seven of the MESSAGe program at the University of Washington. This was done during the program's field camp just as every cohort has done since the program's inception. Instead of doing only 100 counts, five groups each did approximately 200 counts each. The grains were not all counted on a single transect, but on multiple. Every half meter, a grain was counted, and when the whole transect was used, it was moved downstream by half a meter, and then counts resumed. Transects were placed on channel bars. The intermediate axis of the grain is measured and recorded. Fines were counted, but not measured. In total, 920 grains were counted, not including fines. Approximately two hours were spent for five groups to count 200 grains each.

Since the same site has been used to do cobble counts each year since 2012, these additional data

can be used to compare with photogrammetry results and to assess annual variation. Because some slightly different conventions were used for early surveys, I limit my comparison to 2016, 2017, and 2018.

2.1.5 Channel transects from DSM and Lidar

I used ArcMap to extract cross sections from the DSM created as described above.

The most-recent lidar data I can use to build comparison cross sections is the October 2007 1-meter Mount Rainier lidar set. Unfortunately, the park-wide 2012 lidar dataset for Mount Rainier just barely excludes the Nisqually River adjacent to Longmire. Even though the comparisons are 11 years apart, it may be helpful to see how a DSM generated using photogrammetry can compare to a low resolution lidar dataset. I accessed and downloaded the 2007 Mount Rainier lidar dataset through the Washington Department of Natural Resources lidar portal. Five cross sections were chosen to represent this reach of the Nisqually and were placed across the reach. The transects can be seen in Figure 8.

3.0 Results

The main products produced with this project include a point cloud, an orthophoto and DSM generated from the point cloud, automated grain size distributions from images of the orthophoto, and cross sections extracted from the DSM.

3.1 Digital images and models of the field site

The first model produced in this process is a dense point cloud of the Nisqually Channel adjacent to Longmire. The point cloud is produced using Pix4D and took approximately one day to process and create. The point cloud is produced by aligning 359 photos gathered in the field. The amount of area covered is approximately 888,000 ft^2. The GSD (ground sampling distance) for the point cloud is 1.07 cm. The GSD is the minimum size of an object that the point cloud can resolve.

Produced from the dense point cloud, the orthophoto is created. This orthophoto was produced in approximately 3 hours using Pix4D. The total area included is approximately 888,000 ft^2. The resolution of the orthophoto is 1.07 cm per pixel.

The DSM (digital surface model) is also produced from the point cloud, and at the same time as the orthophoto. The DSM took approximately 3 hours to process in Pix4D. The total area is approximately 888,000 ft^2. The resolution is 1.07 cm per pixel. The DSM can be seen in figure 9.

Depending on the resolution and scale of the project, and computer power, an experienced user can create these models in 24 hours. Pix4D is user friendly and there is an option to select all preferences, such as the quality of the point cloud, for the models before they are processed. The point cloud, orthophoto, and DSM can then be created in one step. Preferably, the program would run overnight, with results ready in the morning.

3.2 Grain Size Distributions

I compared grain size distributions from manual cobble counts collected in 2016, 2017, and 2018 to each other and with grain size distributions determined automatically by two different image processing scripts on six sample areas from orthophoto of the same location taken in November 2018.

In total, 853 counts were used for 2018, 670 counts for 2017, and 529 counts used for 2016. In general, the channel bed is well-graded; however, in subchannels that are active in higher stages of flow, there are many patches of fine material that are poorly graded. When comparing the grain size distributions of the manual cobble counts done from 2016-2018, 2016 and 2017 are almost identical. The D50 of 2016-2018 is 115 mm, 100 mm, and 70 mm, respectively. 2018 seems to be slightly finer, although not by much. When comparing the D84 of the manual counts, the 2018 and 2017 are most closely related, with 2016 having a higher D84. This is still in line with the channel fining from 2016 to 2018.

A grain size distribution plot for DGS can be seen in Figure 10 When the grain size distributions are plotted for the DGS results, they mostly take a similar curvature. It is unknown how many grains are counted in each sample area because the DGS scripts do not have an output for the amount of grains counted. There is some variability between grain size distributions when looking at the finer grains, but as the grain sizes get larger, the variability goes down. The maximum grain size counted is close to 1.5 meters while the smallest is approximately 16 mm.

A grain size distribution plot for BASEGRAIN can be seen in Figure 11. BASEGRAIN has little variability between its grain size distribution curves as compared to DGS, and in general, the curves look similar. BASEGRAIN also seems to have trouble counting grains smaller than 45 mm because there are no grains below that threshold that are counted. BASEGRAIN also seems to have trouble detecting larger grains and is capped around a grain size of 750 mm. The number of grains counted in each sample area is unclear; however, the grains that are detected can be seen on the image that is being processed.

When DGS and BASEGRAIN are compared to each other, DGS clearly has more variability and can detect small grain sizes as opposed to BASEGRAIN. BASEGRAIN also does not detect grains that are large, say 1 meter wide, whereas DGS does detect the largest grains. As can be seen in Figure 12, the D50 for DGS was generally lower than the D50 for BASEGRAIN, likely because DGS can detect small grains. The D84 for DGS is also generally lower than that of BASEGRAIN, likely because DGS can detect the smaller grains in the sample areas. BASEGRAIN seems to have the most limited application because it can only detect grains between 45 mm and 750 mm, while DGS can detect grains that are as small as 16 mm and as large as 1.5 meters.

As can be seen in figures 13 and 14, the automated grain size detection methods give results that suggest the sediments in the channel are coarser than the data from the manual cobble counts, with BASEGRAIN giving the coarsest and DGS giving a grain size distribution that is only slightly coarser that produced by the manual counts. The manual D50 ranges from 70-115 mm while the DGS D50 ranges from 96-175 mm. BASEGRAIN, on average, has a coarser D50, ranging from 140-190. Figure 14 also shows little to no overlap for the D50 and D84 between the automated and manual cobble counts, showing that this technique needs more refinement.

3.3 Cross Section comparisons

I produced five different cross sections with each cross section having a transect of both the lidar dataset and the DSM dataset. An example of the cross section comparison can be seen in Figure 16. What is seen immediately is that the DSM transects are at a lower elevation than what they should be by approximately 60 feet. It is unclear why this happened and could be due to the GPS that had been mounted on the camera.

In general, the cross sections produced with the lidar dataset are smoother. The smoothness of the lidar is likely due to the fact that the lidar has a resolution of 1m and less detail can be seen in the channel because of this. Lidar also cannot penetrate the surface of the water, which will give the cross section a smoothed surface because it will only show the elevation of the surface of the water rather than showing the depth and elevation below the water.

The cross sections produced from the DSM are highly detailed and show minute differences in the channel topography. Each DSM cross section has approximately 6000 data points, making them highly detailed. Near the banks of the cross sections, though, the data begin to become inaccurate, most likely because no detailed photographs were taken of the banks and up the banks.

It is difficult to compare the cross sections derived from structure from motion with other cross sections derived from lidar because the lidar dataset is from 2007 for this section of the Park. This leaves the accuracy of the cross sections from photogrammetry unknown; however, it is plain to see that they are fairly similar in shape to the 2007 lidar cross sections, with minor oddities, such as small spikes in the channel and inaccurate representations of the banks. These spikes may be large woody debris or artifacts from the software. They are higher resolution than the 2007 Mount Rainier Lidar set, and the active channels can be clearly seen. Channels that are active at higher stages can also be seen as shown in Figure 15.

4.0 Discussion

4.1 Grain Size Distributions

Is this photogrammetric method for calculating grain size distributions accurate enough to replace traditional cobble counts in the field? There are some advantages, but the limitations may outweigh the benefits; however, there may be some promise in certain applications using these methods. DGS has proved to be fairly accurate in getting a GSD comparable to manual cobble counts, although slightly coarser. If refined, I believe that DGS can be used to gather GSDs of riverbeds rather accurately if grain sizes of 11 mm and below are irrelevant to the application.

One of the more problematic issues in this study when using photogrammetry for structure from motion is the use of ground-based photos. Even with an extension pole, it was difficult to minimize the obliqueness of the photos. If the photos had been taken by UAV (drone), the process of creating the point cloud may have been easier and the results might have been better. When photos are taken at higher elevation, the images capture greater area from a vertical look-direction. This enables the software to align photos correctly, and when a dense point cloud is created, there is minimal raying of objects. When a photo is captured at an oblique angle, the

camera cannot pick up how far back an object may extend, and thus Pix4D tries to estimate the depth. This depth estimate leads to an effect than can severely change the shape of the object, making it extend into the photo. The more oblique the photos in the photoset, the more common and extensive the raying.

The comparison of grain size distributions, both manual and digital, has proved to be somewhat difficult because the manual cobble counts and the software each give a different range of grain sizes. For the field counted cobbles, 2018 is the only year that grain sizes over 320 mm were actually measured, so it is difficult to compare to the digitally derived grain size distributions. When the digital grain sizes were derived, even the largest grains (up to 1400 mm) were counted. With regard to fine particles, image analysis from the orthophoto cannot resolve grain sizes under a certain threshold. For DGS, that minimum threshold is about 11 mm. For BASEGRAIN, the minimum size is approximately 45 mm. The field-counted data distinguishes grains larger than 2 mm. To compare among data sets, I truncated the manual cobble counts at 11 mm and 320 mm. At 11 mm and below, and 320 mm and above, the grains were disregarded and ignored: this way, both the automated and manual counts can be compared to each other.

The primary reason that image analysis scripts are not picking up smaller grains is because resolution of the orthophoto is not high enough. When creating the orthophoto using Pix4D, the highest resolution settings were used, but that gave the orthophoto a resolution of only 10.07 mm/pix. That means that a single pixel was 1 cm across, but many of the grains were smaller than that. One way to get around this is to not use an orthophoto produced with a point cloud. When a point cloud is produced, the resolution is reduced. Instead, to get maximum resolution, a single photo taken perpendicular to the ground using a digital camera would be best. Another issue is that a grain needs to have a certain number of pixels to be considered a grain. For example, BASEGRAIN needs at least 23 pixels for a grain to be counted. This is, however, a problem with the orthophoto, and not the software. The software is meant to analyze high-resolution photographs. Even an average smartphone has a good enough camera to produce images to analyze sand. The example photos provided with the software have resolutions of 0.5 mm/pix, nearly 20 times higher resolution than the orthophoto. This approach is not optimized for field-scale cobble counts.

Even if the grain size distributions are coarser than what is actually in the channel, the photogrammetry method could be useful to pick up sediment bulges over time. These bulges can change the channel gradient and channel elevation, and the D50 can be 1-2 orders of magnitude finer than ambient channel material (Hoffman, 2007). Since DGS has no trouble picking up coarse material, this bulge detection could be a fairly easy task. Another advantage of using an orthophoto is that a grain size distribution could be gathered using the entire reach or parts of the channel instead of just a small section. To get the GSD for an entire reach, the channel would need to be divided into grids with each grid producing an automated GSD. The GSD's of the grid would have to be averaged and that product would be the GSD for the whole reach. If one did want an accurate grain size distribution of a small part of the channel, they could mount a camera to the end of a telescoping pole and take a shot straight down. This single photo of the area desired would be used and would produce an automated GSD instead of an orthophoto. As long as enough grains are in the photo, the software should give an accurate representation of the grain size distribution.

If I were to do this process again with the knowledge that I now have of the software, I would

spend a whole day out in the field gathering a photoset, another day loading that photoset into a structure-from-motion program and running it overnight to produce an orthophoto and DSM, and then another day running images from the orthophoto through automated grain size detection software. In total, three days of work. The software and equipment to get the end product is expensive as well. Pix4D itself costs $5000-$7000 for a license. A standard license for ArcGIS runs from $3000-$4800 for a yearly subscription. MatLab runs at a slightly cheaper price of $2000, and Adobe Lightroom is a subscription service with just a $10 subscription needed. Just about any camera can get this job done so costs range widely. Costs can easily reach $15k just in terms of software needed to complete a project like this.

4.2 Cross Sections

The three options to gather cross sections along the Nisqually River adjacent to Longmire are with a total station, with lidar or with the method I used, creating a DSM with photos through SfM. Each has its caveats. In this situation, a total station can survey only one transect at a time, whereas with a lidar or DSM dataset, there is an unlimited number of transects that can be made and it is easy to create as many transects as needed. A total station is extremely accurate, though, and can measure the channel under the water surface as well. Lidar can be highly accurate as well but to do a lidar survey, the costs are high. Lidar is expensive to produce, and the survey takes a snapshot of the topography at that time. It is thus costly to do yearly lidar surveys. A DSM like the one done for this project is easy, inexpensive, and fast to produce, if the software is available. One caveat is that that DSM will not measure the terrain, but any surface. This limitation means that it will not model the topography under the water just like lidar ,and it will show vegetation in the final product. When producing the DSM, it is also important to get good coverage of the entire channel and the banks, otherwise they will not show up in the DSM.

The digital surface model of the study reach shows fine-scale changes in the channel topography, and separate channels can be seen in Figure 9. These separate channels may be active only at high stages of flow and can be differentiated from the active channel. The only drawback as seen in the cross sections is that photogrammetry surveys cannot measure the channel topography underneath the surface of the water, as total station can. The advantage of using photogrammetry instead of a total station is that photogrammetry will allow one to create a DSM of an entire reach, and a cross section can be taken anywhere along that reach, whereas a total station can measure only one transect at a time.

Because of the ten-year difference in time that these datasets were collected, I do not expect the DSM-derived cross sections to exactly reproduce cross sections extracted from the 2007 lidar. The topography of the channel of the Nisqually River changes rapidly because of all of the sediment being aggraded into the channel. The large sediment supply gives the Nisqually River its braided form. In short, the active channel in 2007 has likely shifted in the years since then.

Because the river is so dynamic, photogrammetry offers significant advantages of an aerial lidar survey. Doing a photogrammetric analysis is quick and inexpensive; therefore, reaches can be modeled often with acceptable accuracy. The only drawback is that photogrammetry cannot cover large areas, such as the 2008 park-wide lidar but would be used for site-specific analysis.

Even though photogrammetry cannot measure the channel under the water surface, I think its applications can still be very useful. Photogrammetry can allow a quick analysis of an entire

reach with higher accuracy than what the Park has available currently. It can also accurately measure width, water level, and surface shape, which all have their own applications in studying imminent threats within the Park.

Just as with the grain size distributions, the process of developing a DSM and using ArcMap to extract cross sections can take upwards of three days and uses much of the same software. The advantages are that photogrammetry is relatively inexpensive to do, the DSM has a high resolution, and a high number of cross sections can be extracted from a single DSM. One disadvantage, though, is that the DSM cannot measure the topography of the portion of the channel that is underwater. Lidar has many of these advantages as well; however, it can be a costly product. The Park paid $10k for the 2007-2008 Park wide lidar survey (Kenyon, *pers. comm.)*. Unless funding is allocated to the Park to do these surveys, they cannot afford to do them every year. The Park currently uses total stations to gather cross sections, but this process can also be time consuming for how little data is retrieved. Only one transect can be done at a time, and to get more transects takes more time to survey. However, total stations are highly accurate and can measure the active channel.

5.0 Recommendations

After evaluating photogrammetric methods to produce an orthophoto and DSM for the purpose of extracting grain size distributions and cross sections of the Nisqually Riverbed adjacent to Longmire in Mount Rainier National Park, I think that these methods have a time and place to be practiced, but only in certain situations.

For cross sections, if time and costs are limiting factors and certain established cross sections need to be measured, then a total station is likely the fastest way to get accurate results. If more than a few cross sections need to be measured and time is not a limiting factor, I think that a DSM produced using photogrammetry is a good choice. If a DSM is produced, then many different cross sections can be created, and as shown in this project, the DSM can yield high accuracy as well, as long as the banks are covered well enough during the photoset gathering, and appropriate ground control is used to georeference the images. This may be the best method to use when river stages are low enough to survey the whole channel with a photoset, as a DSM cannot interpret topography underneath the surface of the river. If time and cost are not limiting factors, then lidar surveys are the best way to go, depending on lidar resolution. Because lidar surveys are expensive, the Park cannot afford one every year. An option might be to do a photoset of certain reaches of certain rivers each year, such that high accuracy models can be produced for every year.

For grain size distributions, I would likely go about the process in a different way. Rather than creating orthophotos for the digital grain size analysis, I would gather single photos of the channel that are shot with a telescoping pole, looking straight down. These photos can be used as input into DGS to get an accurate representation of the grain size distribution, as opposed to using an orthophoto created from a point cloud. When the point cloud is created from a photoset, each of the photos loses resolution, which lowers the resolution of the orthophoto. This prevents DGS from detecting finer grains. If a single photo can be used to accurately represent a grain size distribution, then this method may even be able to replace manual cobble counts, as it would save significant time. Furthermore, this approach could reduce potential sample bias introduced from an individual picking grains, since software would not show a bias unless coded into the

detection algorithms. Further experiments would need to be done to show the accuracy of using a single photo taken with a commercial grade camera compared to manual cobble counts, and I think that is the next step in determining grain size distributions with automated grain detection methods. One could theoretically walk on to a river bed, take a photo of it with a pole, and walk to a computer with the proper software to get a grain size distribution in minutes. One can even take photos while walking up a river bed, and when grain size distributions are plotted using the software, one may be able to see how that grain size distribution changes, possibly detecting sediment pulses in as little as an hour, depending on the scale of the pulses. If, in any case, finer grains are irrelevant and only the coarser grains need to be analyzed, then an orthophoto can also be a reasonably accurate way to get a GSD. But even then, this is a much longer process compared to getting GSDs from a single photo.

6.0 References Cited

AgiSoft PhotoScan Standard (Version 1.4.4) (Software). (2018). Retrieved from http://www.agisoft.com/downloads/installer/

Anderson, S.W., P.M. Kennard, and J. Pitlick, 2013, Geomorphic assessment of significant sediment loading in Tahoma Creek: Science Brief, Mount Rainier National Park, 2 p..

Beason, S.R., 2017, Change in glacial extent at Mount Rainier National Park from 1896-2015: Natural Resource Report NPS/MORA/NRR-2017/1472, National Park Service, 98 p..

Beason, S.R., L.C. Walkup, and P.M. Kennard, 2015, Aggradation of glacially-sourced braided rivers at Mount Rainier National Park, Washington: Summary report for 1997-2012: Natural Resource Technical Report NPS/MORA/NRTR-2014/910, National Park Service, 166 p.

Bullock, A.B., K. Bacher, J. Baum, T. Bickley, and L. Taylor, 2007, The flood of 2006: 2007 Update: Unpublished Report, Mount Rainier National Park, 43 p..

Buscombe, D., D. M. Rubin, and J. A. Warrick (2010), A universal approximation of grain size from images of noncohesive sediment, J. Geophys. Res., 115, F02015, doi:10.1029/2009JF001477.

Buscombe, D. (2013), Transferable wavelet method for grain-size distribution from images of sediment surfaces and thin sections, and other natural granular patterns. Sedimentology, 60: 1709-1732. doi:10.1111/sed.12049

Carbonneau, P.E., Lane, S.N., Bergeron, N.E. 2004. Catchment-scale mapping of surface grain size in gravel bed rivers using airborne digital imagery. WRR 40(W07202).

Detert, M., Weitbrecht, V. (2012). Automatic object detection to analyze the geometry of gravel grains – a free stand-alone tool. River Flow 2012, R.M. Muños (Ed.), Taylor & Francis Group, London, ISBN 978-0-415-62129-8, pp. 595-600.

Detert, Martin & Weitbrecht, Volker. (2013). User guide to gravelometric image analysis by BASEGRAIN.

Driedger, C. L., and P. M. Kennard. 1986. Ice volumes on Cascade Volcanoes: Mount Rainier, Mount Hood, Three Sisters, and Mount Shasta. United States Geological Survey Professional Paper 1365, 28 p.

Fiske, R.S., C.A. Hopson, and A.C. Waters, 1963, Geology of Mount Rainier National Park, Washington: Professional Paper 444, United States Geological Survey, 93 p..

Hoffman DF, Gabet EJ. 2007. Effects of sediment pulses on channel morphology in a gravel-bed river. Geological Society of America Bulletin 119: 116–125. DOI. 10.1130/B25982.1

Legg, N.T., A.J. Meigs, G.E. Grant, and P.M. Kennard, 2014, Debris flow initiation in proglacial gullies on Mount Rainier, Washington: Geomorphology, Vol. 226, pp. 249-260.

Mattinson, J. (1977). Emplacement history of the Tatoosh volcanic-plutonic complex, Washington: Ages of zircons. Geological Society of America Bulletin, 88(10), 1509-7606-88-10-1509-17320.

Pix4D: Professional photogrammetry and drone-mapping (Version 4.4.4)(Software).(2018) retrieved from https://www.pix4d.com

Sisson, T. W., J. W. Vallance, and P. T. Pringle (2001), Progress made in understanding Mount Rainier's hazards, Eos Trans. AGU, 82(9), 113–120, doi:10.1029/01EO00057.

Snavely, S.N. Seitz, R. Szeliski (2008), Modeling the world from internet photo collections. International Journal of Computer Vision, 80, pp. 189-210

Wolman, M. G. (1954), A method of sampling coarse river-bed material, Eos Trans. AGU, 35(6), 951–956, doi:10.1029/TR035i006p00951.

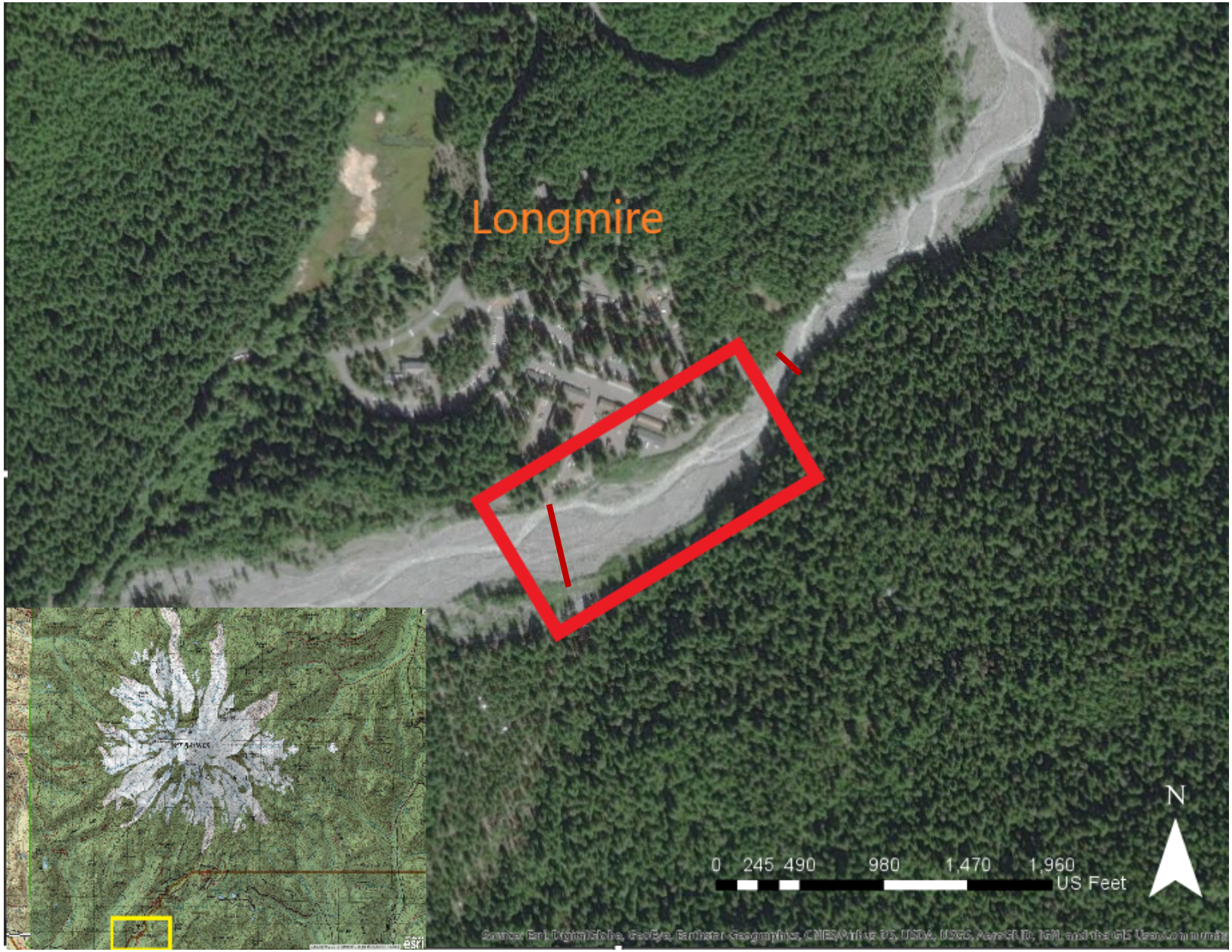

Figure 1: Site map showing where Longmire and the site are located within Mount Rainier National Park. This figure also shows how the Nisqually River narrows and broadens out due to the geology of the surrounding area. The red box indicate the field site. The two red lines indicate the width of the Nisqually, showing how drastically the river widens out from where it is confined.

Figure 2: A picture of the field site itself, across the river from Longmire, looking west. Taken October 2016. Trees on closest bank are approximately 10-12 feet tall.

Figure 3: The Nisqually River during the November 2006 flood, nearly wiping out the emergency operations center in Longmire (Beason, et al., 2015).

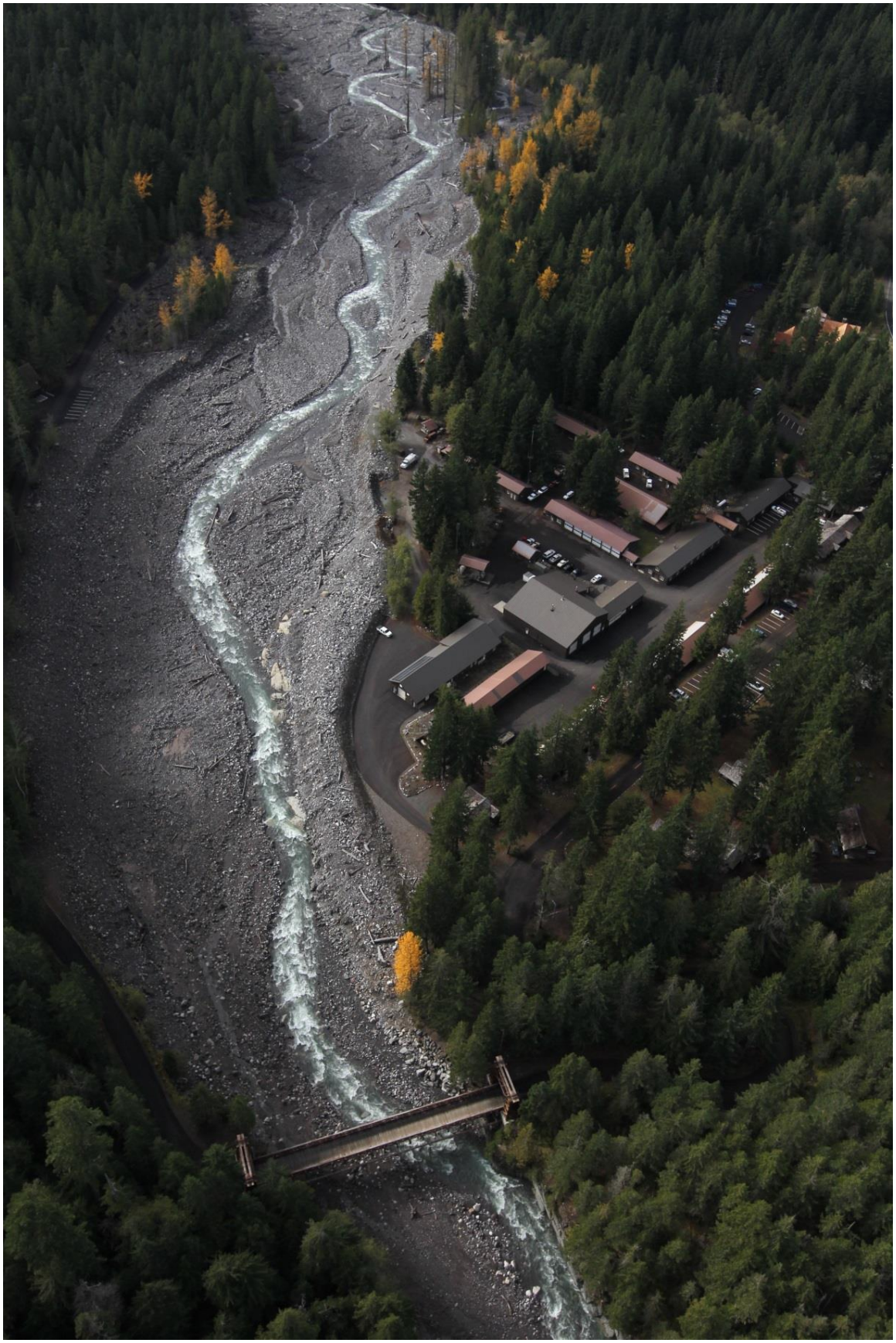

Figure 4: A 2010 aerial photograph of Longmire and the Nisqually River as seen from above. The constructed levee can be seen on the right bank. This photograph shows that the Nisqually is higher in elevation than Longmire itself. (Credit: Dean Koepfler, The News Tribune, Tacoma,

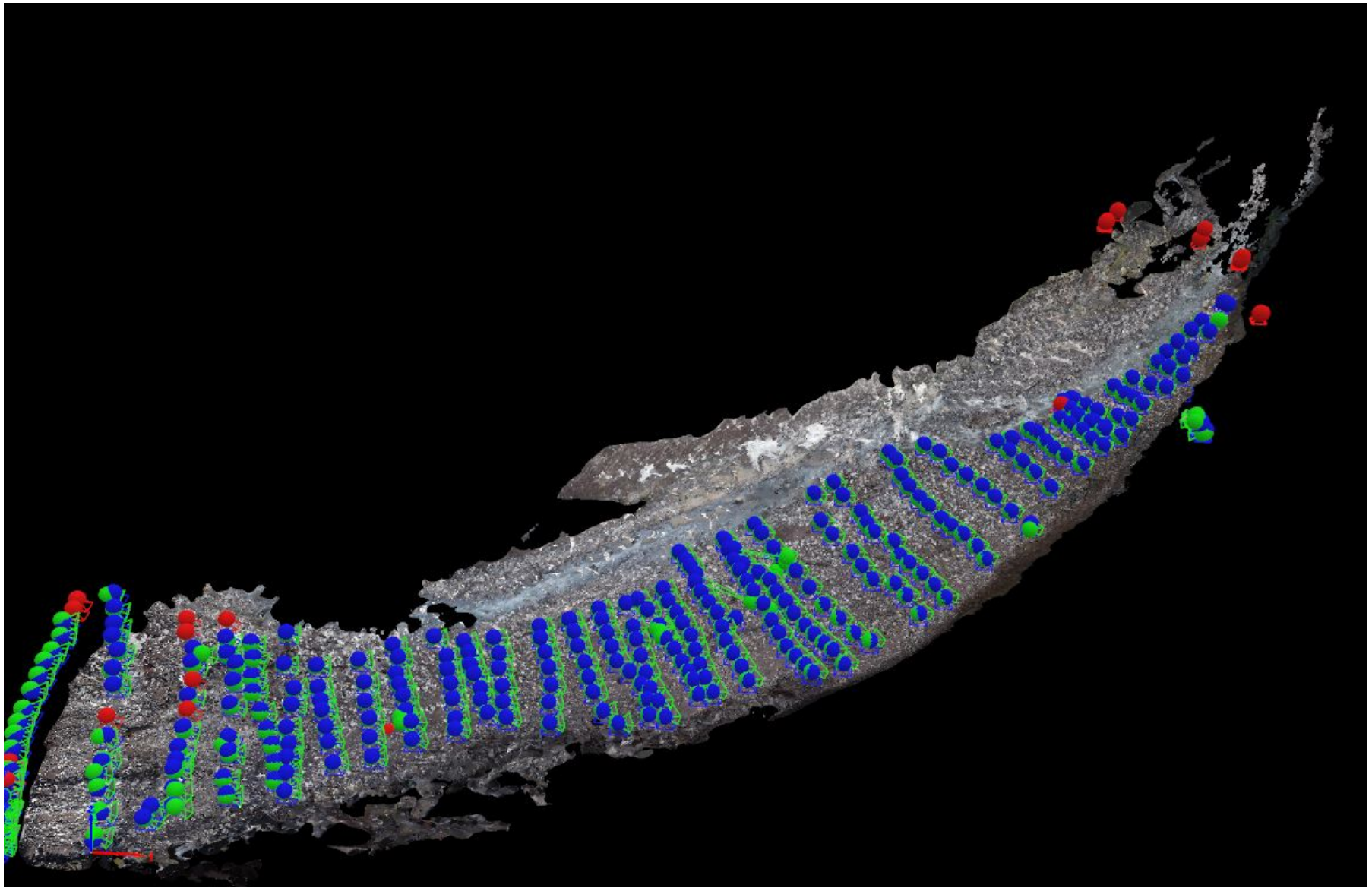

Figure 5: The point cloud model that was generated from the photoset. This picture also shows blue dots that represent where photos were taken. The dots clearly show the zig-zag pattern that was done to ensure proper coverage of the entire channel. The channel is approximately 1000 feet in length and north is toward the top of the picture.

Figure 6: A zoomed shot of the point cloud that was made using Pix4D. Resolution is 10.07 mm/pix. The logs in the photo are approximately 20-25 feet in length.

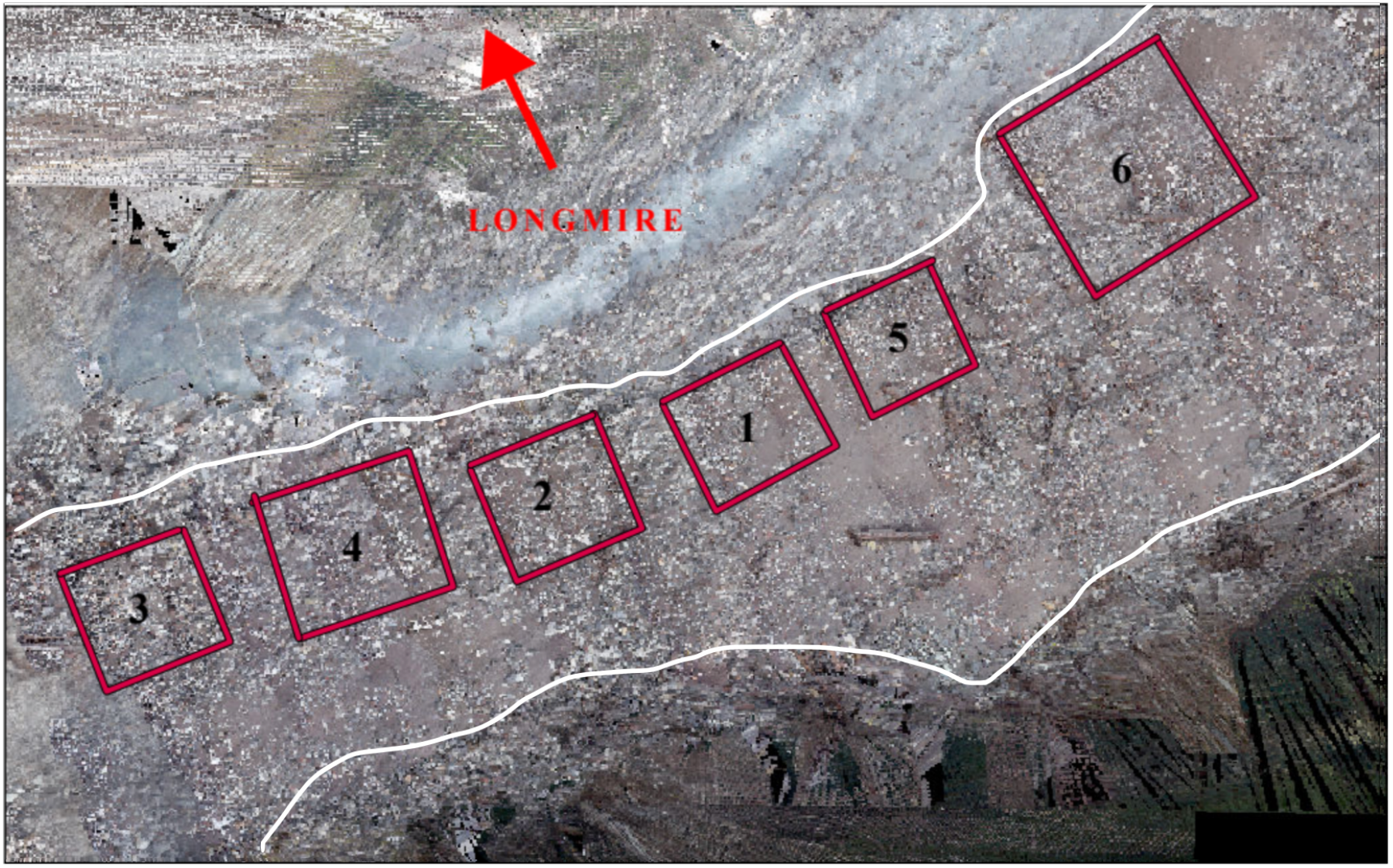

Figure 7: The six sample areas chosen to get grain size distributions. The sample areas are plotted on the orthophoto produced from the point cloud in this figure. The white lines define the functional model.

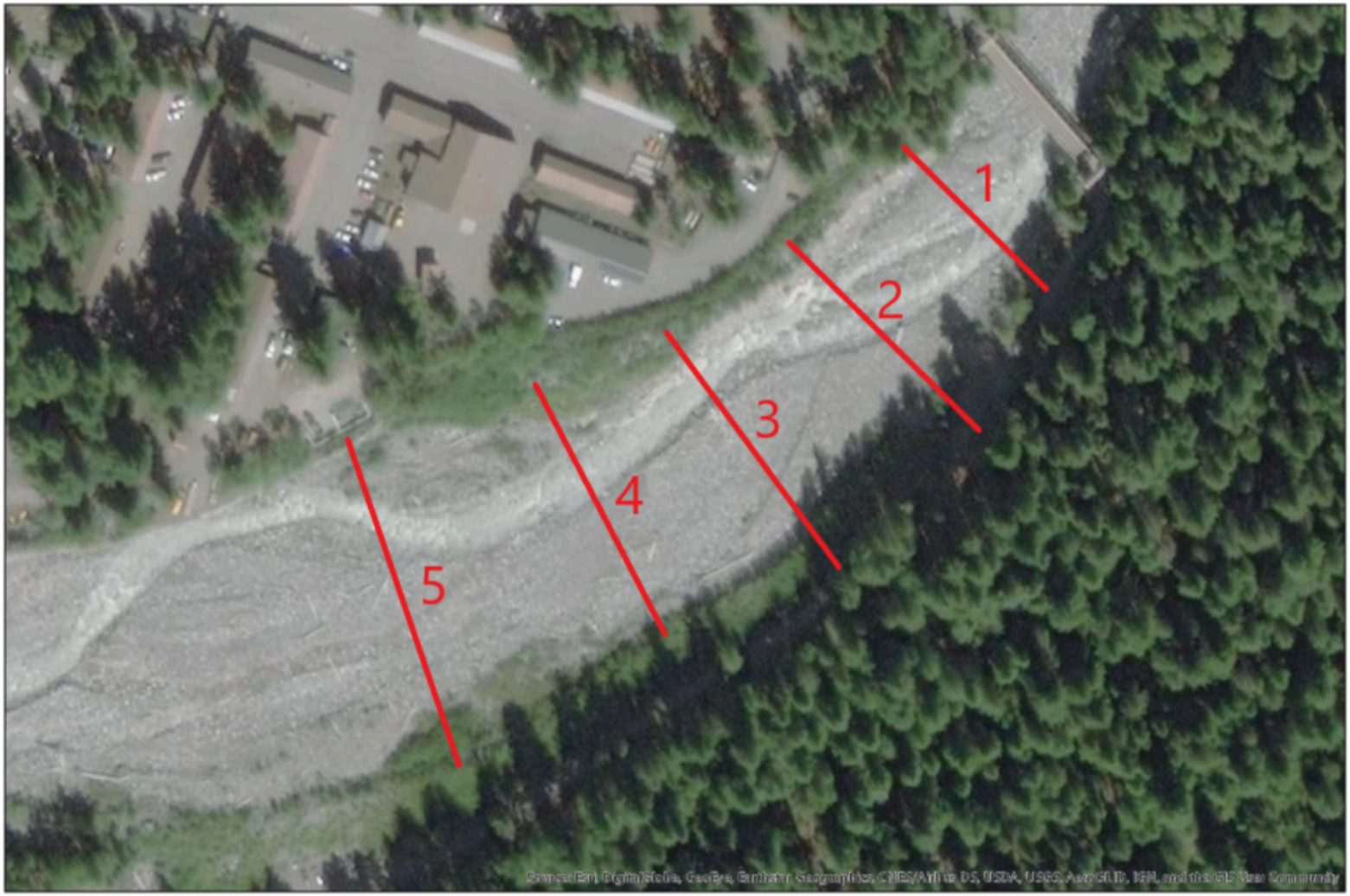

Figure 8 : The five transects chosen for cross sections.

Figure 9: The digital surface model created using Pix4D. Many different channels other than the active channel can be seen.

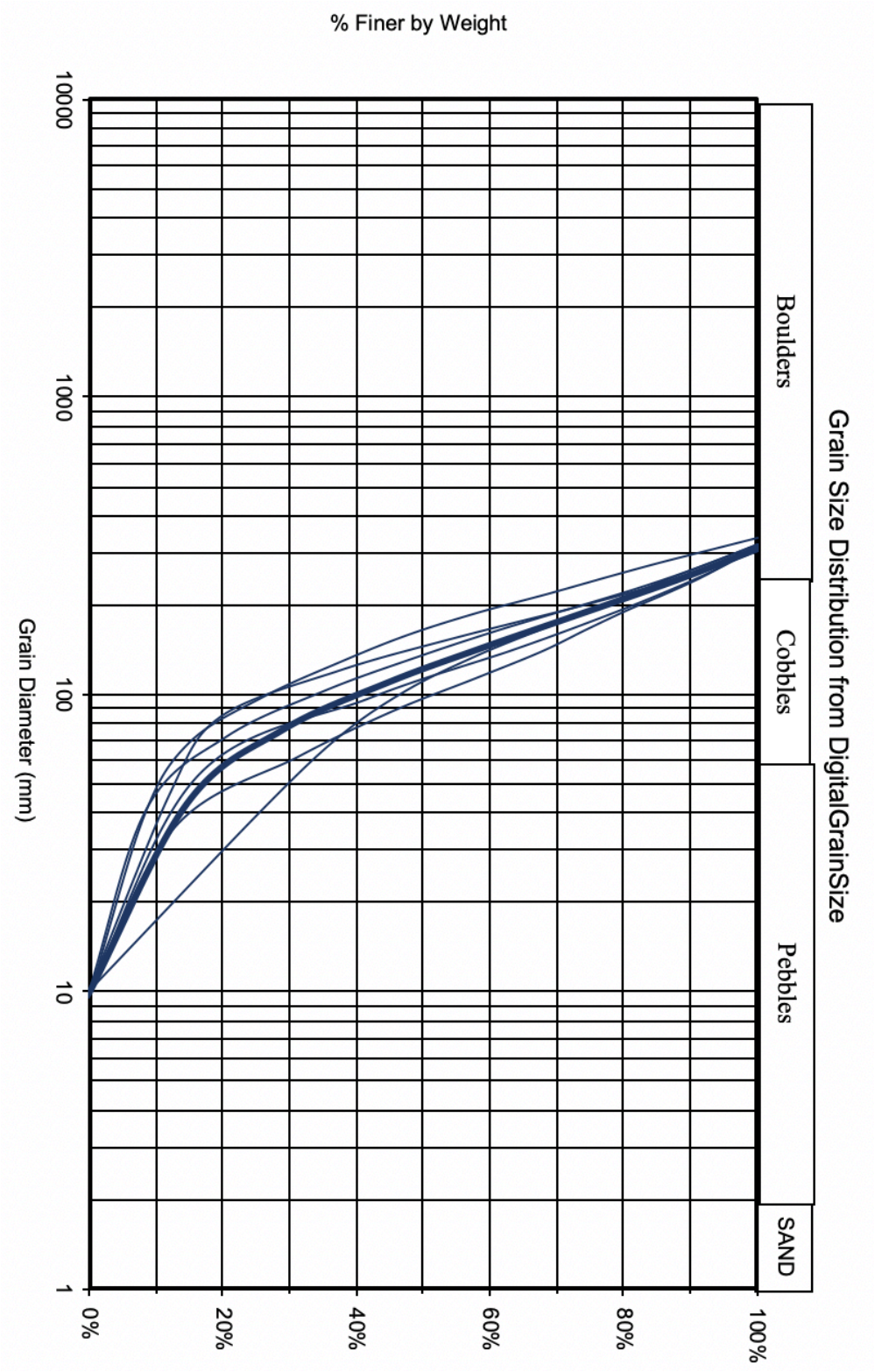

Figure 10: Grain size distribution for the six sample areas using DigitalGrainSize. The bold line is a composite of the six sample areas.

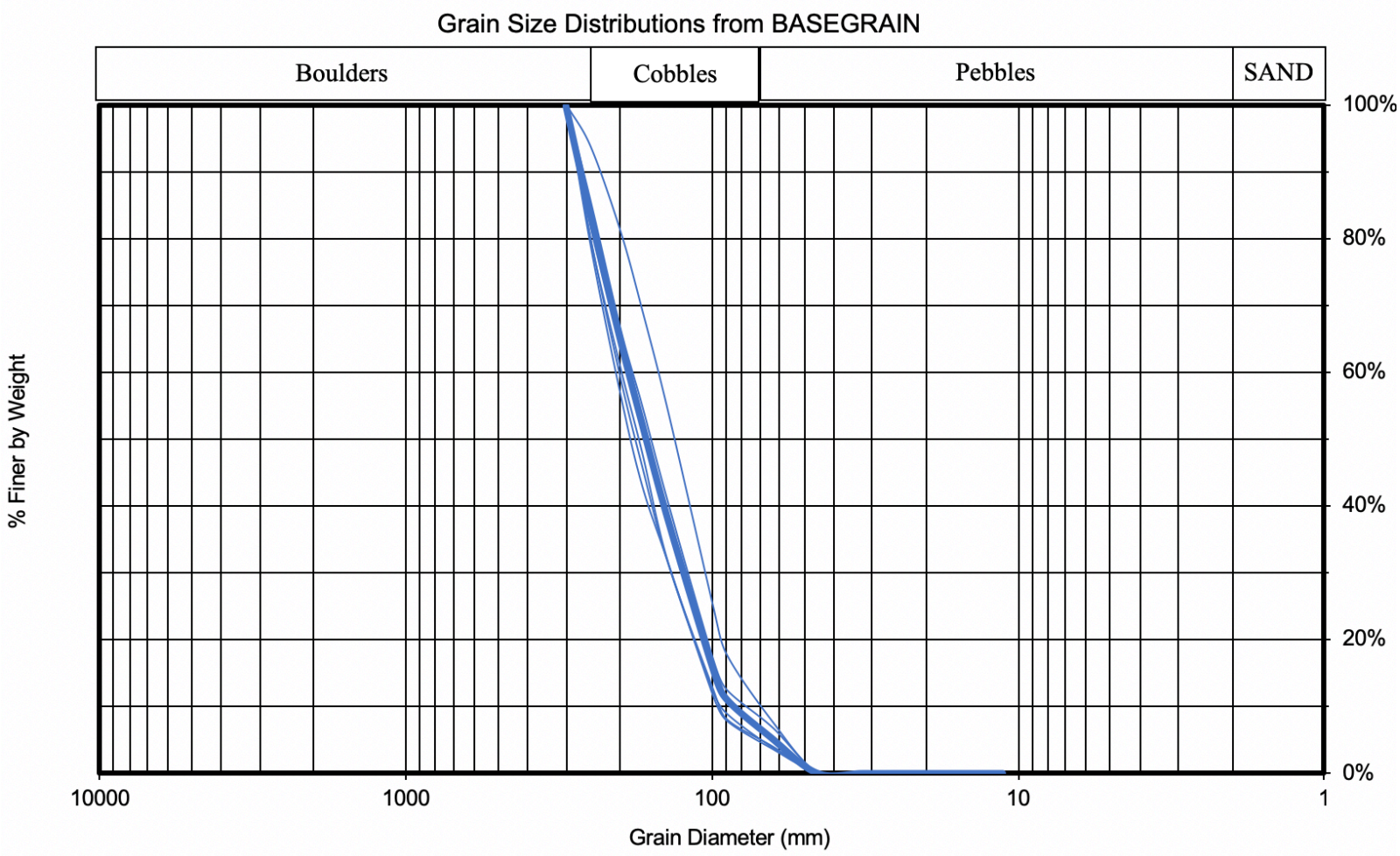

Figure 11: Grain size distribution of the six sample areas using BASEGRAIN. The bold line is a composite of all six sample areas.

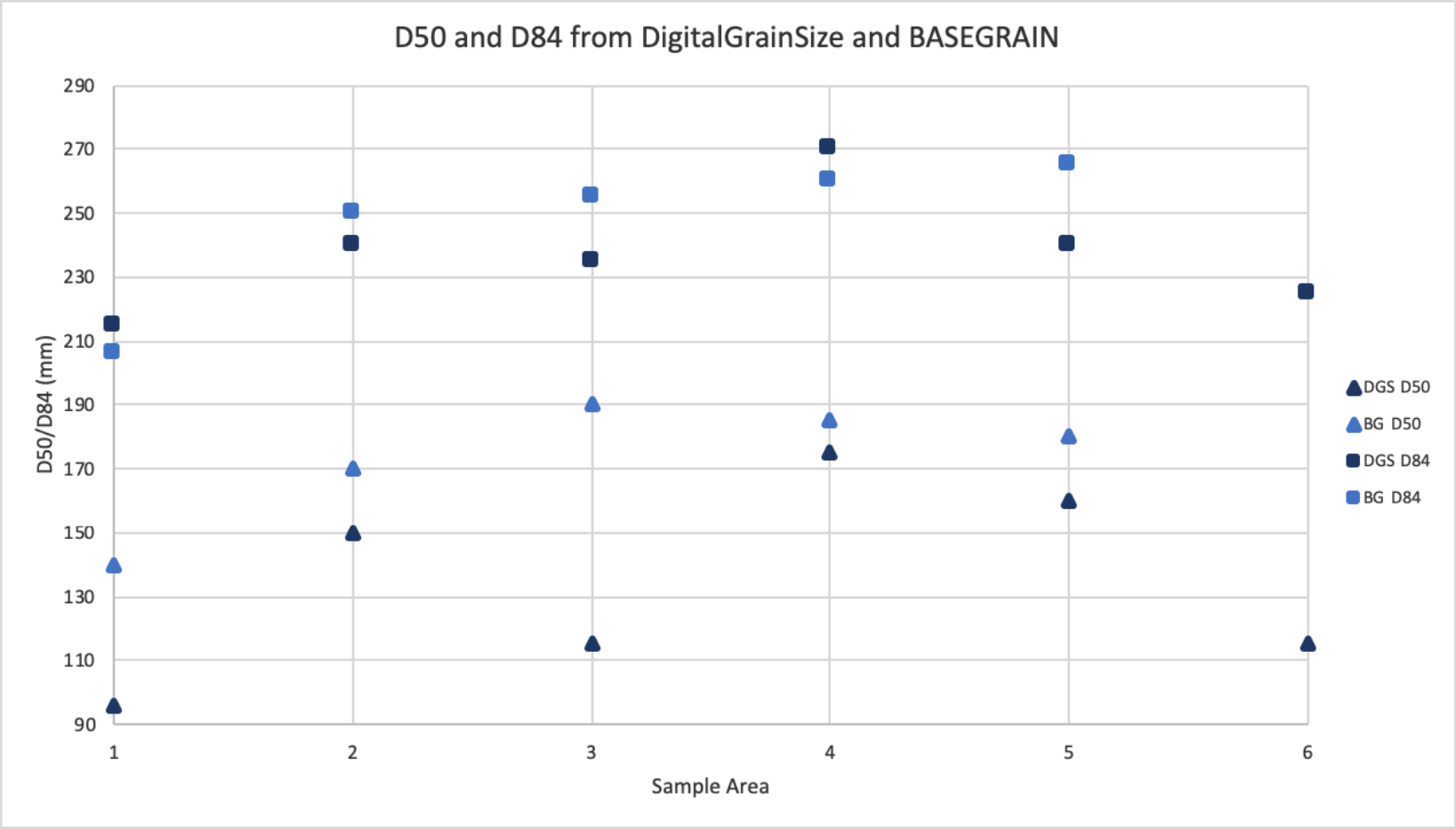

Figure 12: The truncated D50 and D84 from both DigitalGrainSize and BASEGRAIN.

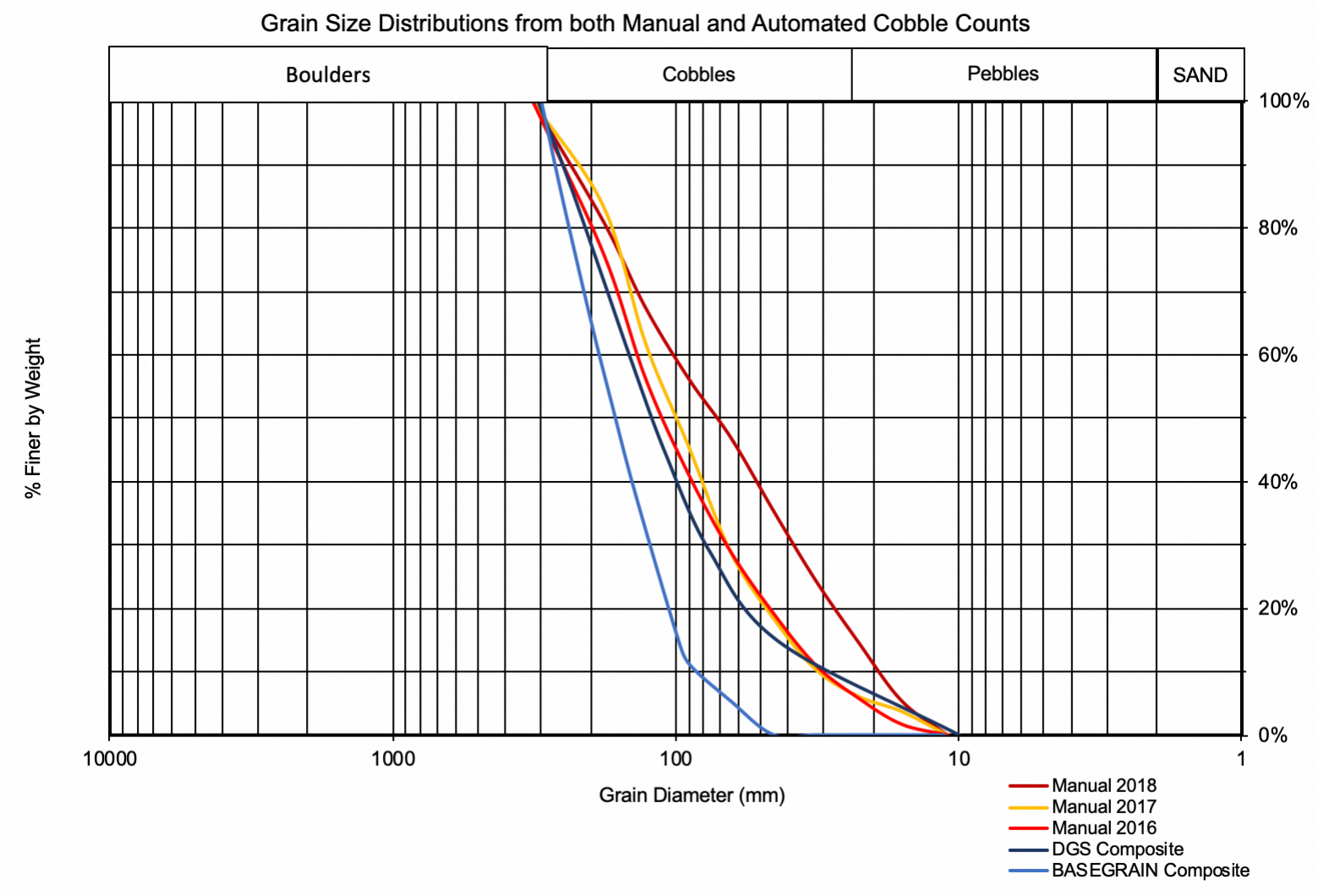

Figure 13: Grain size distributions from both of the automated methods and manual cobble counts from mid-September of three different years. All counts are truncated below 10 mm and above 320 mm. As show here, the 2016 and 2017 years of cobble counts are similar and 2018 is finer, while the DGS counts are slightly coarser and BASEGRAIN is much coarser. The DGS counts also have the same general curve as the 2016 and 2017 manual counts, which shows potential that it can act as a replacement for manual cobble counts.

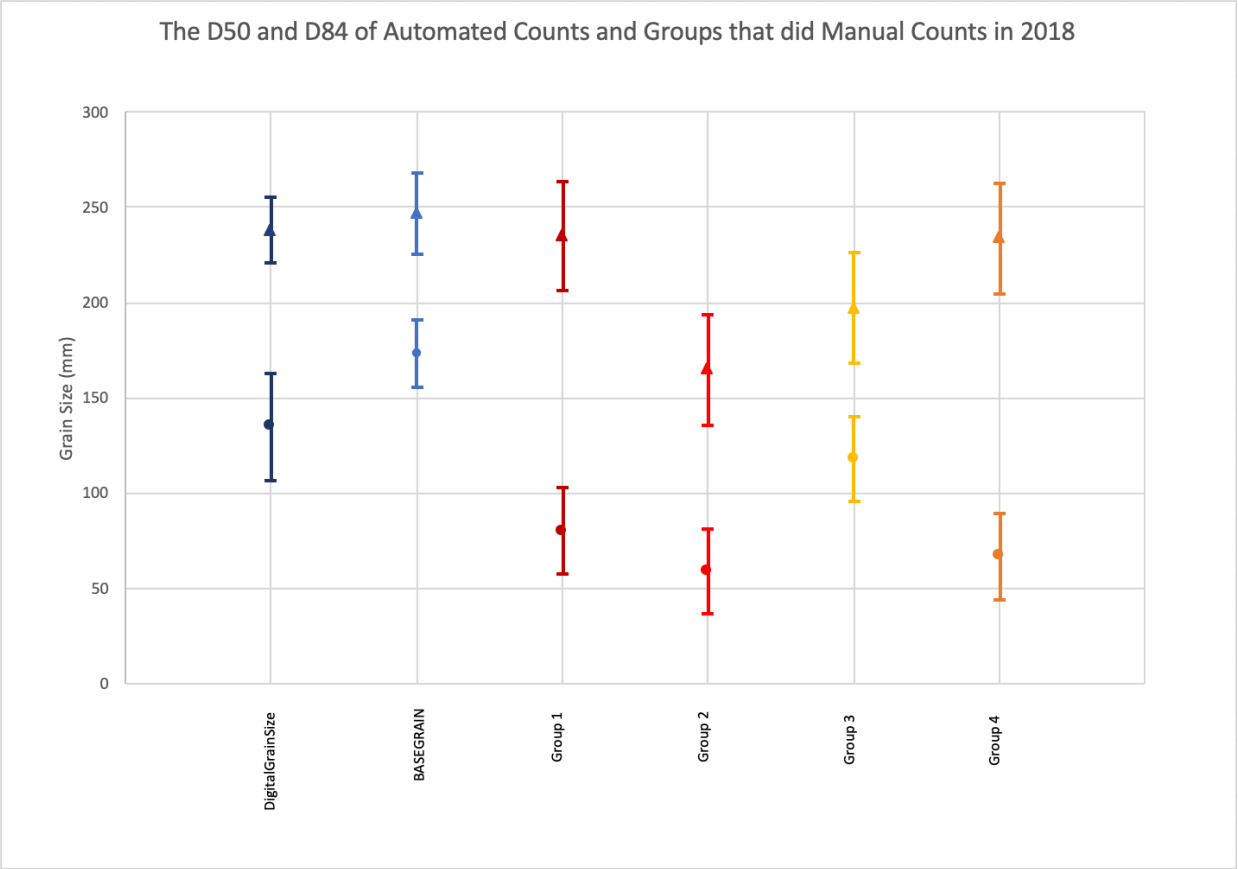

Figure 14: The truncated D50 and D84 as well as the standard deviation of both the automated grain size detection software, as well as the four groups that did cobble counts in 2018. As shown here, the manual counts and the automated counts do not overlap often, proving that this technique still needs to be refined for it to be useful.

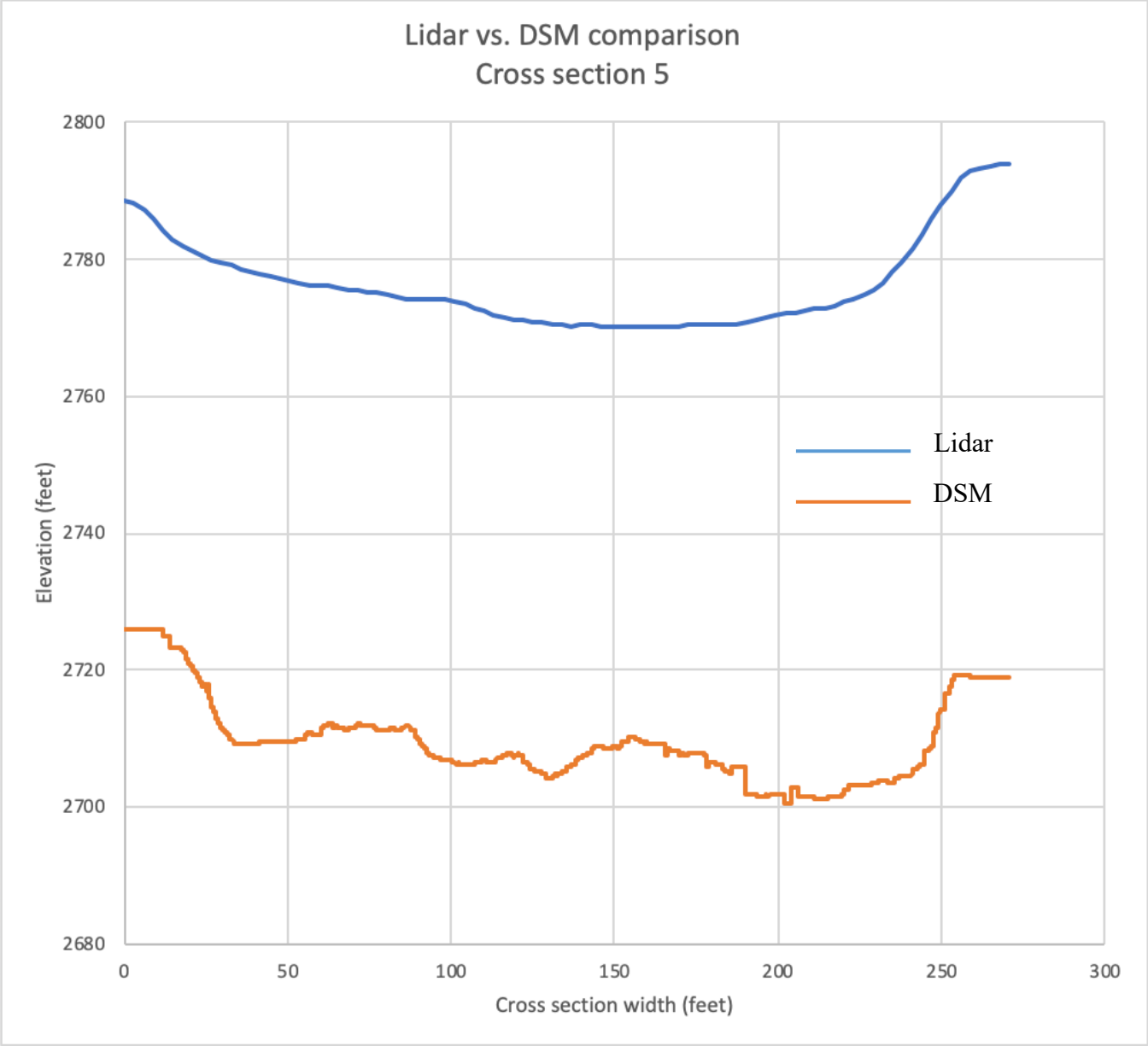

Figure 15: One of the five cross section comparison produced using the 2007 lidar and the DSM generated with Pix4D. Immediately seen is the elevation difference between the two cross sections. This may be due to GPS error but requires further investigation. The high resolution of channel can be seen on the DSM. The lowest elevation channel is was the active channel at the time the photos were taken, with the other channels likely active at higher flows.

8.0 Appendix

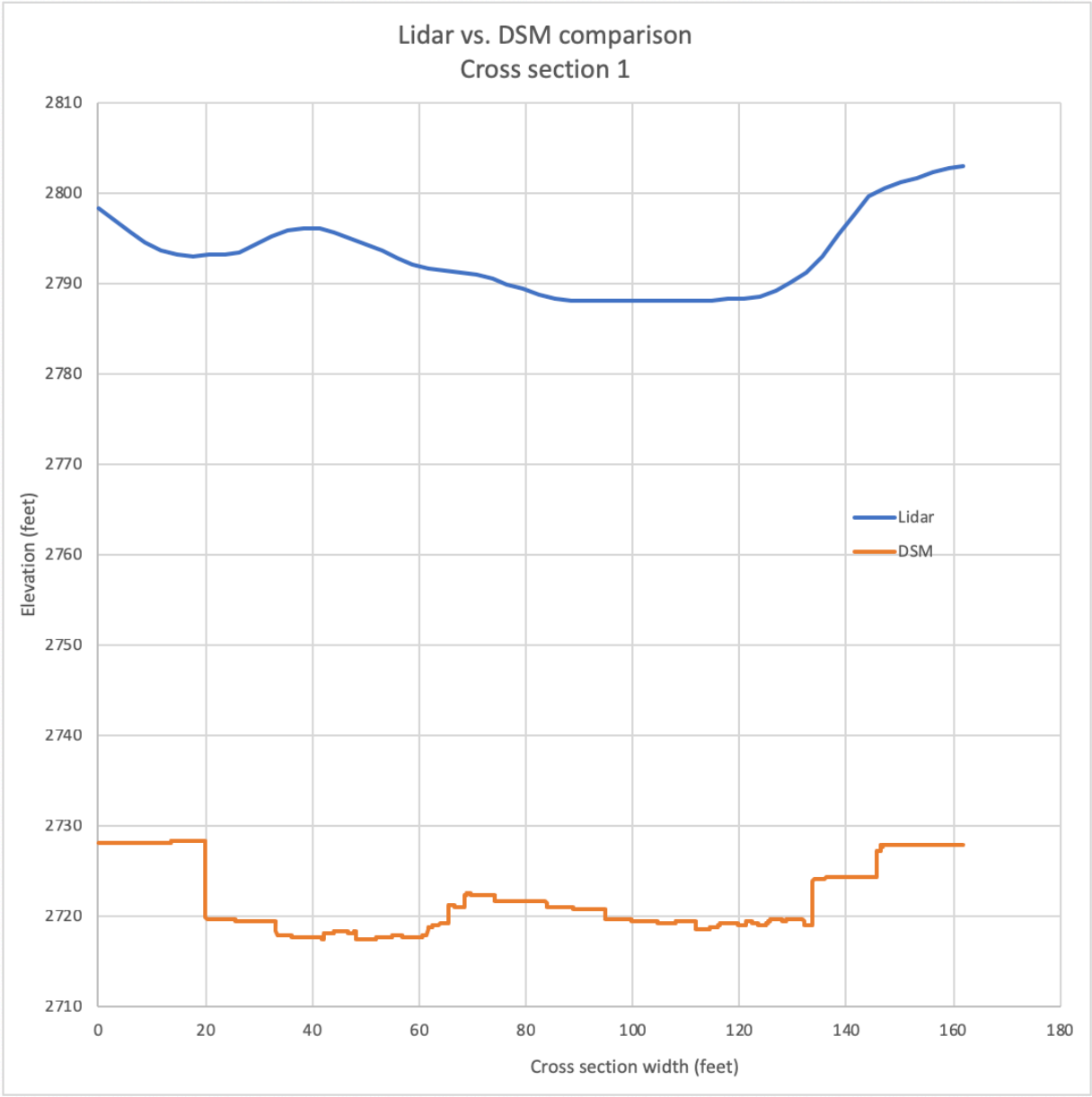

Figure A1: Cross section one comparison between the lidar and digital surface model.

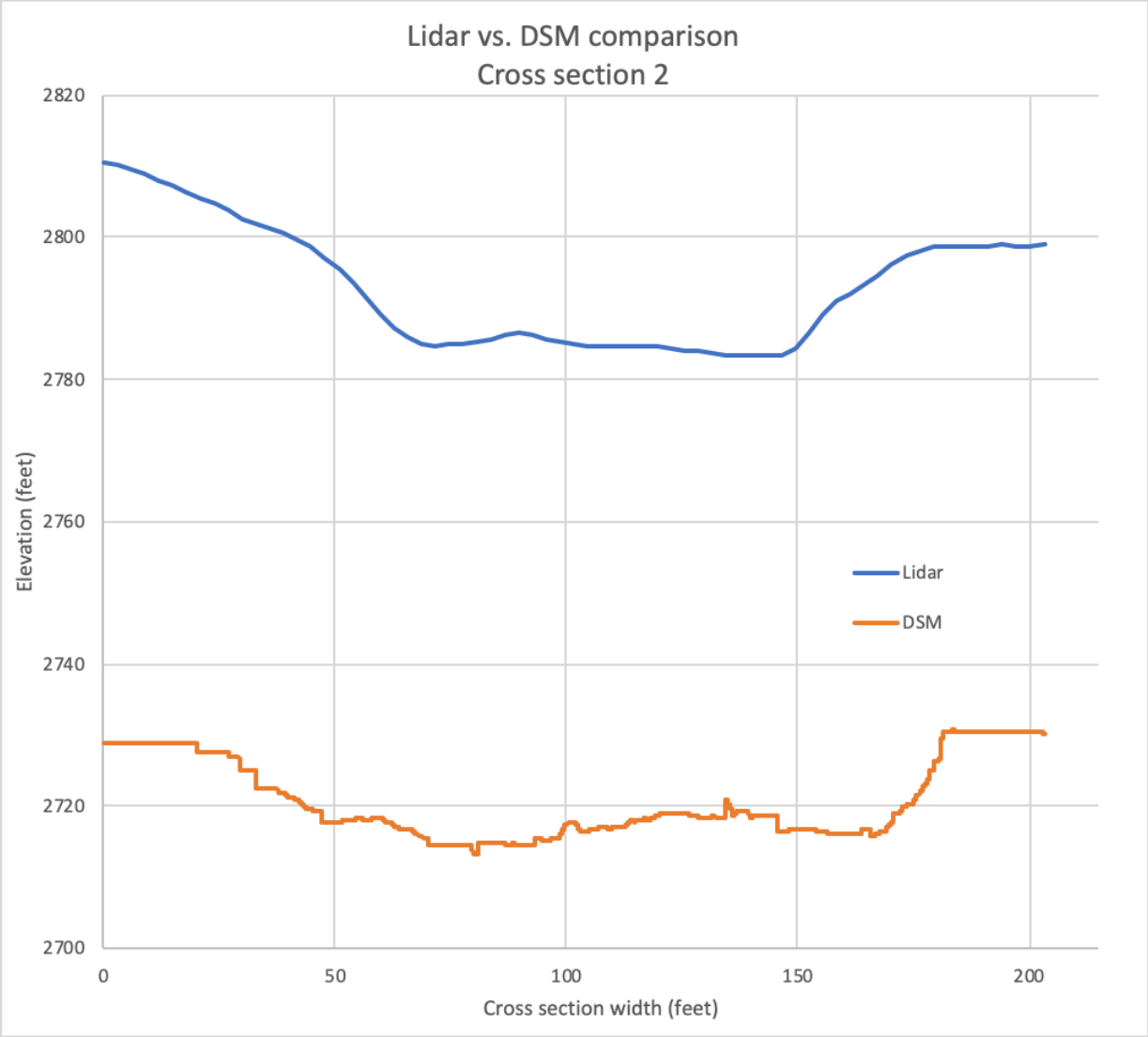

Figure A2: Cross section two comparison between the lidar and digital surface model.

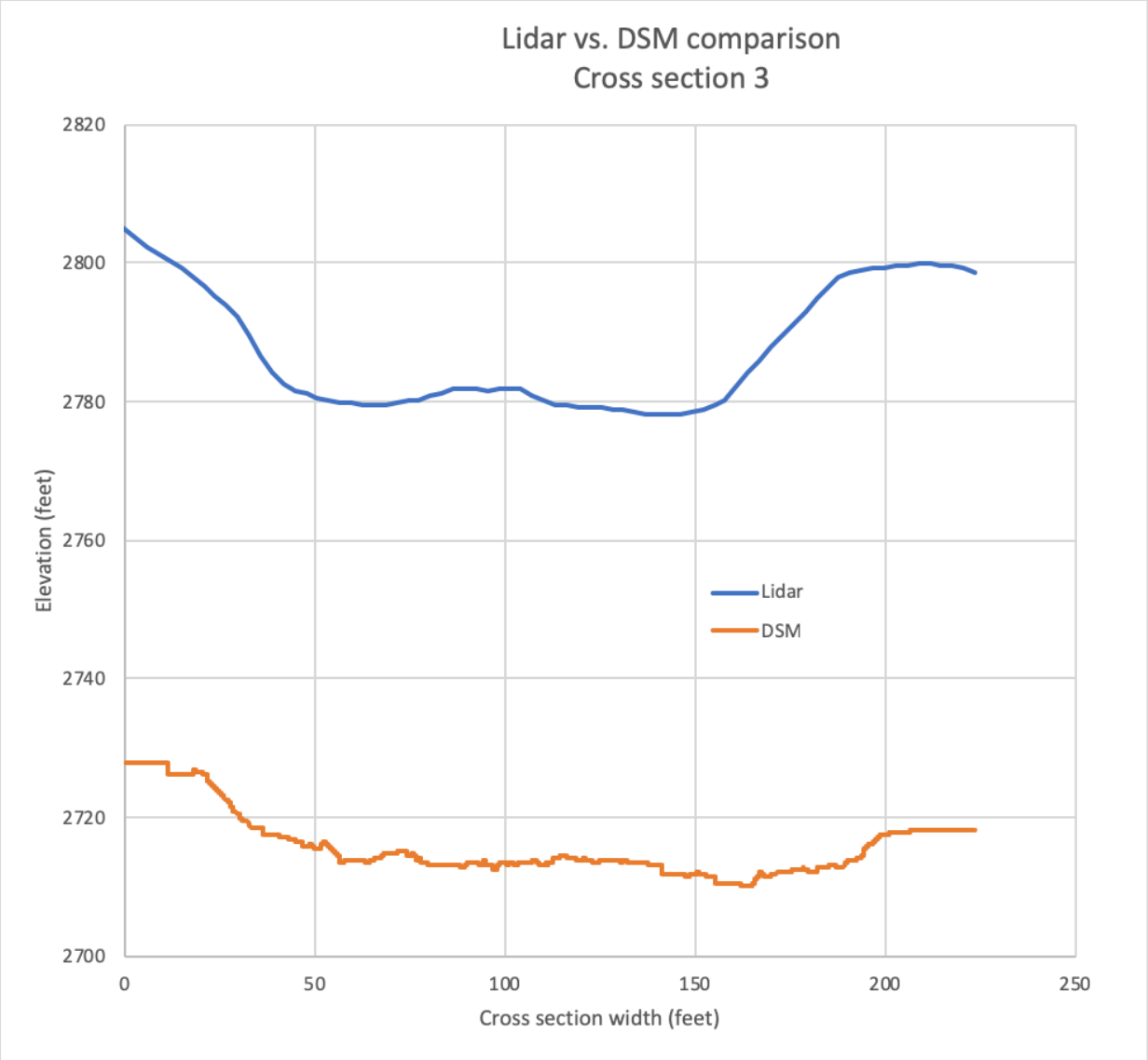

Figure A3: Cross section three comparison between the lidar and digital surface model.

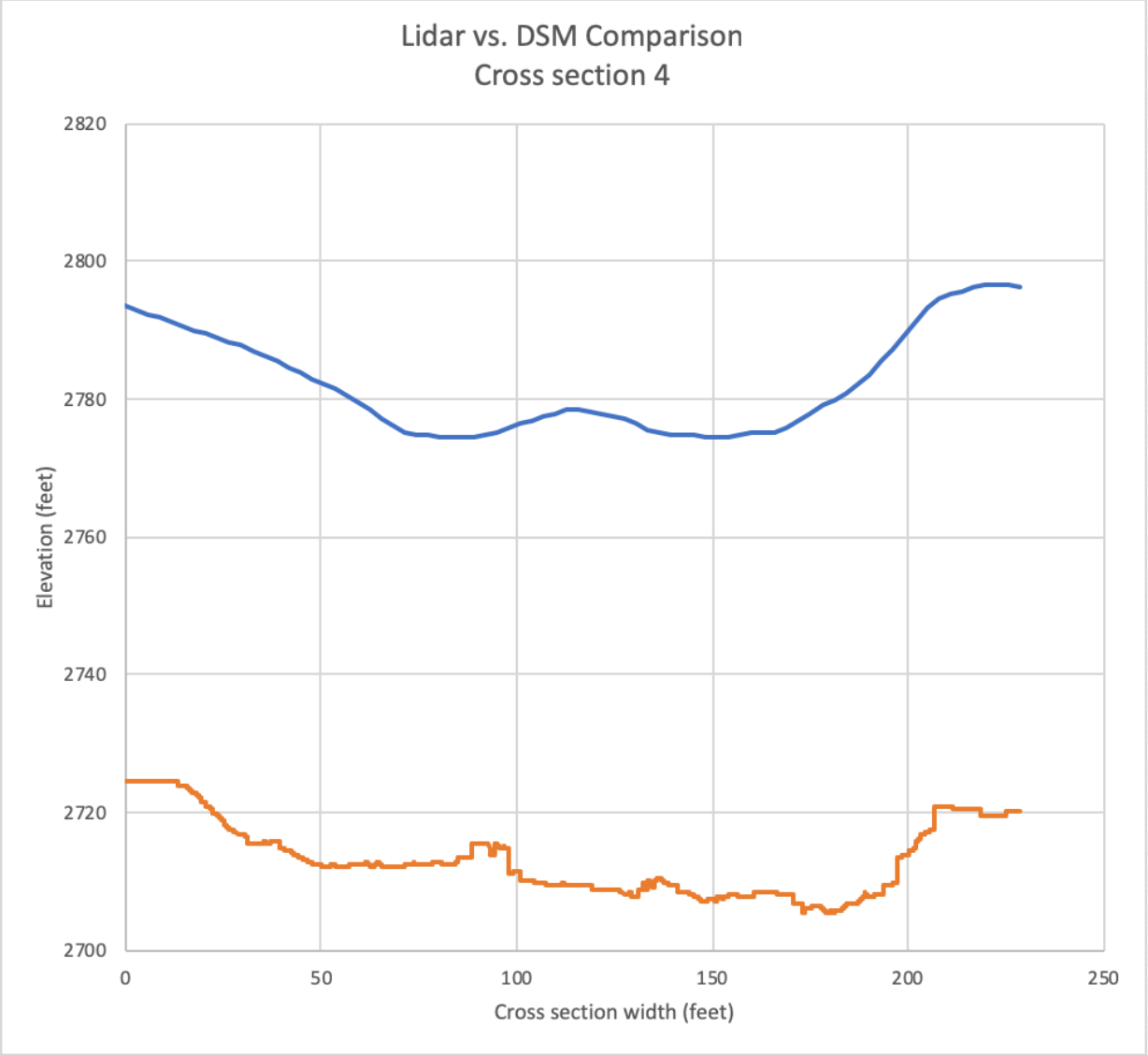

Figure A4: Cross section four comparison between the lidar and digital surface model.

Table A1: The programs used for this project, their uses, and their sources.		
Software	**Description**	**Source**
Pix4D v4.4.4	Generates point cloud, orthophoto, and DSM based on photos	https://www.pix4d.com
ArcMap v10.6.1	Extracts sample areas from orthophoto and cross sections from DSM	http://desktop.arcgis.com/en/arcmap/
Adobe Photoshop v6	Used to convert between formats for image files	https://www.adobe.com/products/photoshop.html
RTKLIB	Extracts GPS coordinates that are aligned with the camera shutter	http://www.rtklib.com
MatLab v9.5	Interface and processing engine that runs the DigitalGrainSize and BASEGRAIN scripts	https://www.mathworks.com/products/matlab.html
DigitalGrainSize v3	A script that performs automated grain size distributions on images based on wavelets	https://dbuscombe-usgs.github.io/DGS_Project/
BASEGRAIN v2.2	A script that performs automated grain size distributions on images based on separating interstices from grain areas	http://www.basement.ethz.ch/download/tools/basegrain.html
Microsoft Excel v16.22	Used to graph and compare grain size distributions and cross sections	https://products.office.com/en-us/excel